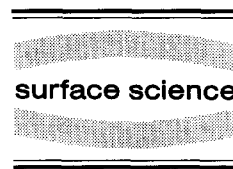




ELSEVIER

Surface Science 337 (1995) 268–277



# Polar surfaces of oxides: reactivity and reconstruction

D. Cappus, M. Haßel, E. Neuhaus, M. Heber, F. Rohr, H.-J. Freund \*

*Physical Chemistry 1, Ruhr-Universität Bochum, Universitätsstrasse 150, 44780 Bochum, Germany*

Received 24 August 1994; accepted for publication 21 November 1994

## Abstract

Polar oxide (111) surfaces are prepared on thin films of NiO, CoO and FeO. In the limit of completely ionic rock salt type crystal structures these (111) surfaces, whether they are oxygen or metal terminated, show a tendency for reconstruction. We show that the unreconstructed polar surfaces are OH covered, and, after OH removal, the surface reconstructs. We show that this is true for NiO(111). For CoO(111) the stability of the oxide film does not allow the removal of OH, so that the reconstruction cannot be observed. The FeO(111) surface is permanently reconstructed and we show that for FeO(111) grown on Fe(110) the surface is not of Fe<sub>3</sub>O<sub>4</sub>(111) type.

*Keywords:* Cobalt oxides; Electron energy loss spectroscopy; Iron oxide; Low energy electron diffraction (LEED); Nickel oxides; Photoelectron spectroscopy

## 1. Introduction

Adopting the extreme view of a completely ionic oxide with rock salt structure, the polar (111) surface of such a material will be thermodynamically unstable due to a divergent surface potential [1–4]. Stabilization is possible by reduction of the surface charge which may occur via various routes. For example, if we would exchange the top layer of an oxygen terminated NiO(111) surface, as shown in Fig. 1a by OH, we would reduce the surface charge per atom from  $-2$  to  $-1$ , thus stabilizing the surface [5,6]. Alternatively, geometric reconstruction of the surface layer can lead to surface stabilization [1,2,6]. The most stable reconstruction of a polar surface of an ionic crystal is, according to Lacmann [1] and to Wolf [2], the so-called octopolar reconstruction as

shown in Fig. 1b. The octopolar reconstruction leads to a  $p(2 \times 2)$  unit cell on the surface and is characterized by the removal of three out of four oxygen ions in the first layer (in the case of an oxygen terminated surface) and one out of four nickel ions within the second layer. The third layer contains then again a complete hexagonally close-packed oxygen layer. A  $p(2 \times 2)$  reconstruction has been observed for ironoxide [7–10] and nickeloxide [6], but only in the latter case there are indications that an octopolar reconstruction has actually taken place. Weiß et al. [7,10] have recently found strong indications on the basis of a LEED [10] analysis and on XPS data [7] that oxidation of iron deposited on top of a Pt(111) single crystal surface does lead to a Fe<sub>3</sub>O<sub>4</sub> surface layer rather than a reconstructed FeO surface. As is clear from the schematic representations of the ideally terminated surfaces in Fig. 2, the Fe<sub>3</sub>O<sub>4</sub>(111) surface and the reconstructed FeO(111) surface would lead to the same LEED pattern, since the reconstruc-

\* Corresponding author.

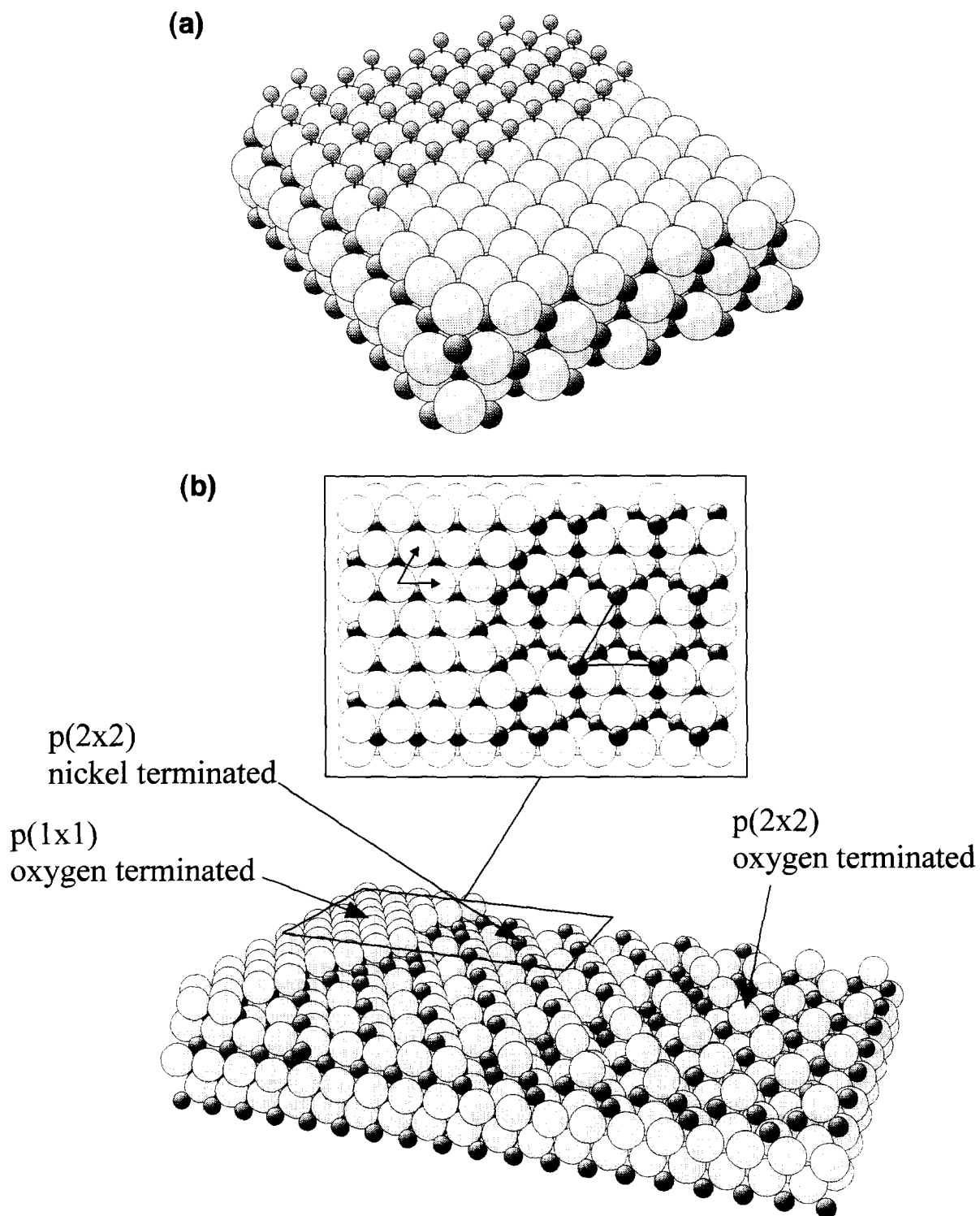


Fig. 1. (a) Schematic representation of an oxygen terminated and OH terminated NiO(111) surface. (b) Schematic representation of an octopolar reconstructed NiO(111) surface. The  $p(2 \times 2)$  octopolar reconstruction involves several layers in the substrate and is shown for two possible surface terminations.

tion would result in a unit mesh of twice the size of the bulk truncated FeO(111) surface [11]. One argument put forward by Weiß et al. [7,10] favoring the spinell surface is the instability expected for FeO under the chosen circumstances (UHV, room temperature) based on the bulk phase diagram [12]. Support for the argument is found in experiments where a Fe<sub>2</sub>O<sub>3</sub> crystal surface reconstructs leading to the same p(2 × 2) pattern which has very recently been identified to be also a Fe<sub>3</sub>O<sub>4</sub> surface [8,11]. Furthermore Weiß et al. performed LEED intensity calculations for several FeO(111) reconstructed surfaces and for an unreconstructed Fe<sub>3</sub>O<sub>4</sub>(111) surface. Best agreement with experimental data was achieved for the Fe<sub>3</sub>O<sub>4</sub> surface [8,10].

In the present study we have investigated the polar surfaces of CoO and of FeO films grown on the respective metal single crystal surfaces with (111) and (110) orientations. We show that CoO(111) grows hydroxyl terminated as in the case of NiO(111). However, the hydroxyl groups cannot be removed by a thermal treatment because the stability of the oxide film is not sufficient. On Fe(110) we grow an ironoxide film with FeO stoichiometry and a Fe 2p XP-spectrum characteristic of Fe<sup>2+</sup>. Electron diffraction yields a p(2 × 2) pattern. We propose that due to the large Fe reservoir, and in deviation to the situation on the Pt(111) substrate, the equilibrium

$$4\text{FeO} \rightleftharpoons \text{Fe} + \text{Fe}_3\text{O}_4$$

is shifted towards the left hand side. It is therefore

very likely that the observed p(2 × 2) superstructure is due to a reconstruction of the above discussed type.

## 2. Experimental

The experiments have been performed in various different ultrahigh-vacuum chambers employing low energy electron diffraction including spot-profile analysis (SPA-LEED) as well as X-ray photoelectron spectroscopy (XPS) with monochromatized Al K $\alpha$  radiation and electron energy loss spectroscopy (EELS).

The single crystal samples (Ni, Co, Fe) were spotwelded to two tungsten wires which were attached to a liquid nitrogen reservoir. With this arrangement temperatures below  $T = 100$  K could be reached. A tungsten filament was mounted behind the sample which could be used for sample heating by electron impact or radiative heating. The samples were cleaned by repeated cycles of etching with Ne ions and annealing. The oxide films have been prepared by oxidation of the metal single crystals ((111) and (110) orientation) in an oxygen atmosphere on the basis of information in the literature [5,13–23]. The Ni oxide was grown by cycles of oxidation with 1000 L (1 L = 10<sup>-6</sup> Torr · s) of O<sub>2</sub> at elevated temperature ( $T = 570$  K) followed by annealing at  $T = 650$  K. These cycles were repeated until the

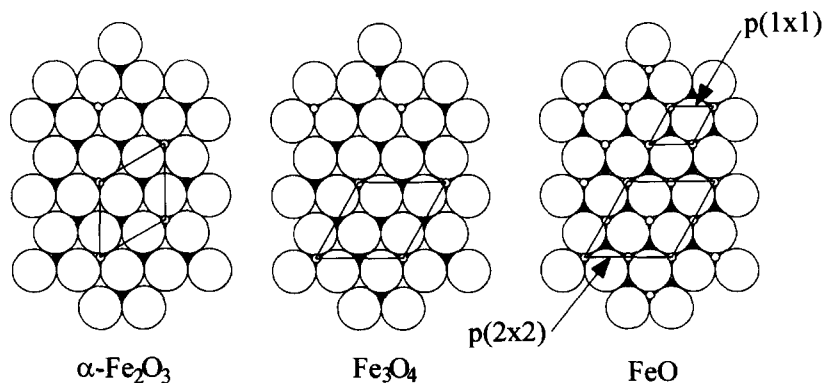


Fig. 2. Schematic representation of ideally terminated iron oxide (111) surfaces: (a)  $\alpha\text{-Fe}_2\text{O}_3$ ; (b)  $\text{Fe}_3\text{O}_4$ ; (c)  $\text{FeO}$ . The unit meshes are indicated. It is clear that the unit mesh on the  $\text{Fe}_3\text{O}_4$ (111) surface creates the same p(2 × 2) LEED pattern as a reconstructed  $\text{FeO}$ (111) surface.

LEED pattern indicated the formation of an ordered oxide film. CoO(111) was prepared by exposing Co(0001) to 10.000 L O<sub>2</sub> at elevated temperatures

(450 K) and subsequent annealing (1 h) at 450 K. The FeO(111) film was prepared in a similar way by oxidation of a Fe(110) single crystal with 4000 L O<sub>2</sub>

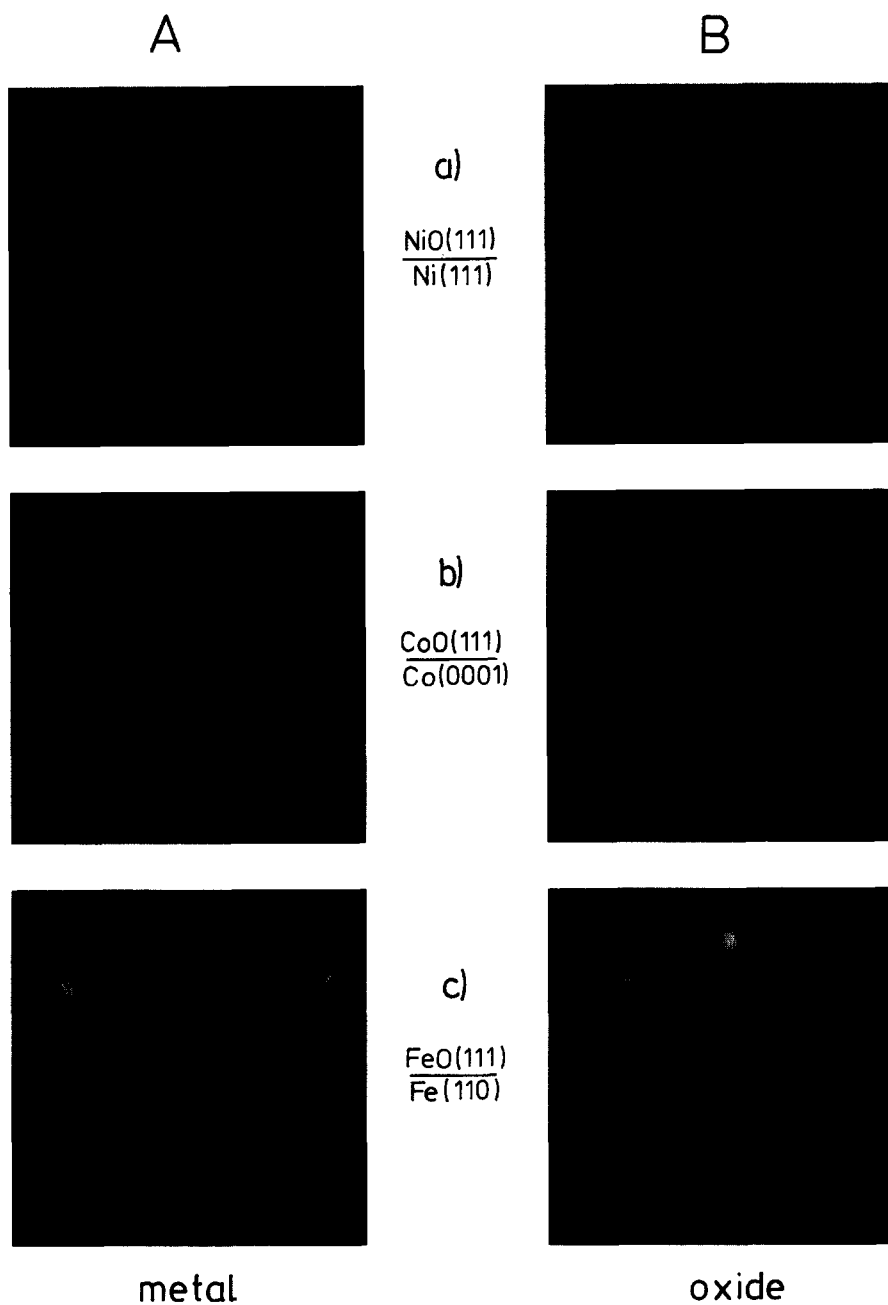


Fig. 3. (a) LEED patterns of a NiO(111) film (A) as prepared on a Ni(111) surface (B) via oxidation. (b) LEED pattern of a CoO(111) film (A) as prepared on a Co(0001) surface (B) via oxidation. (c) LEED pattern of a FeO(111) film (A) as prepared on a Fe(110) surface (B) via oxidation.

at  $T = 600$  K and annealing at  $T = 870$  K for 4 min afterwards.

### 3. Results and discussion

#### 3.1. NiO(111)/Ni(111)

Fig. 3a shows the LEED pattern of a NiO(111) film grown epitaxially on a Ni(111) single crystal

surface. The oxide spots are still considerably broader than the metal reflexes due to the imperfections induced by the large lattice mismatch between metal and metal oxide (18%) [24] but the substrate spots are no longer observed.

The EELS spectra in Fig. 4a indicate the adsorption of considerable amounts of hydroxyl groups by the observation of strong losses, at 460 meV. The OH groups may be partially exchanged through exposure of the surface to D<sub>2</sub>O which leads to an

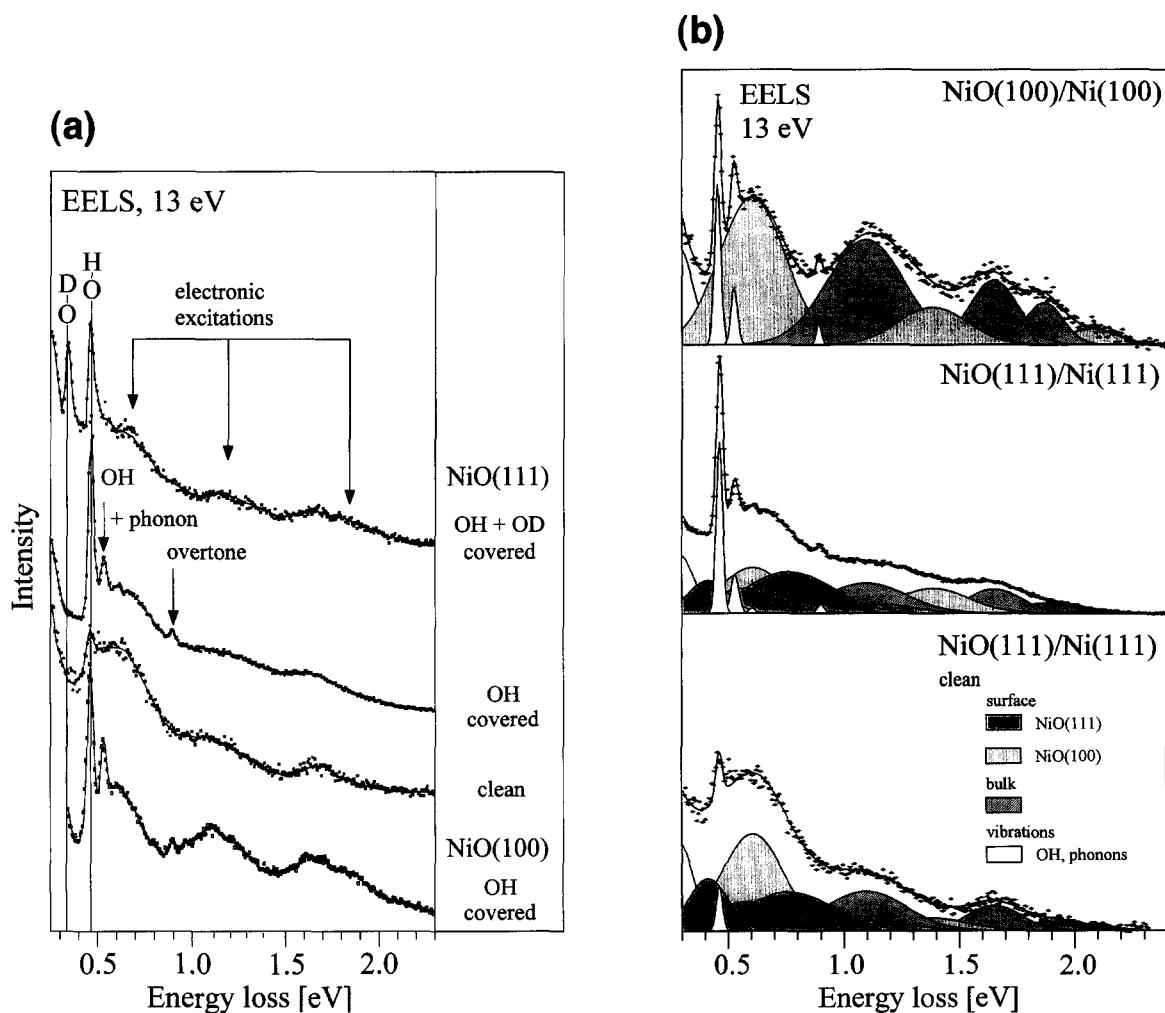


Fig. 4. (a) EELS spectra of NiO(111) surfaces after different preparation conditions. In comparison we show the EELS spectrum of a NiO(100) film at the bottom. (b) Fit to the EELS spectra of NiO(111)/Ni(111) as prepared after removal of OH and of a NiO(100) film according to the bulk and surface concentrations of differently coordinated Ni ions based on calculations by Freitag and Staemmler [26] for d–d excitations.

isotope shift as seen in Fig. 4a. These losses are situated on top of a background of electronic excitations within the NiO band gap as has been previously discussed for the NiO(100) surface by Freitag et al. [25]. In Fig. 4a also the EELS spectrum of the NiO(100) surface is shown. The comparison shows similar but not identical features in the case of the electronic excitations for both surfaces. The reason is twofold: firstly, if the hexagonal (111) surface is OH terminated the Ni ions are all in octahedral environments thus only contributing to the bulk signals present at both (100) and (111) surfaces. Second, if the (111) surface is not OH terminated, but rather reconstructed, a small part of the Ni ions are in a threefold ligand field thus leading to a corresponding surface excitation spectrum different from (100) (fourfold symmetry). All other Ni ions in the reconstructed layer are in environments typical for a NiO(100) surface. From a weighted superposition of the spectra we do not expect enormous differences between the surface excitations on NiO(100) and NiO(111). In Fig. 4b we show fits to the EELS spectra which basically corroborate the above assignments. The fits are based upon a mixture of experimental [5,25] and theoretical [25,26] information. Freitag and Staemmler [26] have calculated excitation energies for Ni<sup>2+</sup> ions in various crystal fields and we have used this as input for our fits.

It was shown earlier that the adsorbed hydroxyl groups lead to a pronounced shoulder in the O 1s XP spectra at approximately 1.5 eV higher binding energy [5] as compared with the lattice oxygen feature.

As monitored via EELS and XPS, the hydroxyl groups can be removed to a large extent by a simple heat treatment. Fig. 4a shows the EELS spectra after removal of the majority of the hydroxyl groups. Due to the larger number of Ni ions in (100) coordination in the reconstructed surface the spectrum is more similar to the one of the (100) surface. In conjunction with this change in composition, we observe changes in the LEED patterns. Fig. 5a shows a two-dimensional SPA-LEED pattern of the oxide film taken at an electron energy of 80 eV. This pattern corresponds to the  $p(1 \times 1)$  NiO pattern in Fig. 3a. The distortion of the symmetry of the pattern is due to the experimental arrangement in the SPA-LEED set up. If the sample is heated to slightly above 600 K we see changes in the intensity distribu-

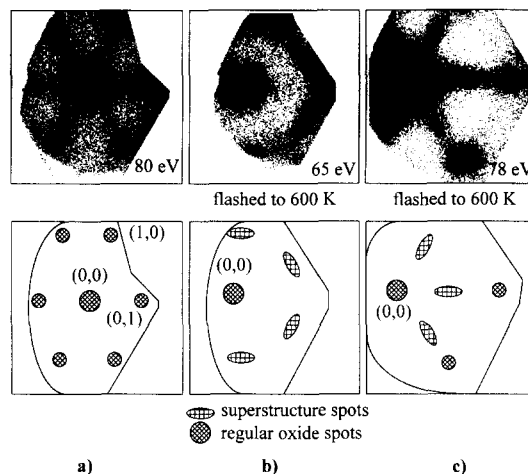


Fig. 5. Two-dimensional SPA-LEED pattern of (a) the  $p(1 \times 1)$ ; (b), (c) the  $p(2 \times 2)$  reconstructed surface at two different electron energies.

tion of the LEED pattern. Figs. 5b and 5c show SPA-LEED patterns taken at two different electron energies because there is considerable variation of spot intensity with electron energy. At 65 eV electron energy the fractional order  $p(2 \times 2)$  spots in the second Brillouin zone are intense, while the fractional order  $(2 \times 2)$  spots in the first Brillouin zone and the integral order spots have very low intensity. At 78 eV electron energy, on the other hand, intense integral order and first order  $p(2 \times 2)$  spots are found. Even though the SPA-LEED patterns are distorted, it is clear that the  $p(2 \times 2)$  NiO spots are not located near the positions of the sharper  $p(2 \times 2)$  O/Ni(111) spots reported in Ref. [6]. Therefore, the  $p(2 \times 2)$  reconstruction is clearly connected with the NiO lattice. A detailed structure determination, however, has not been undertaken yet. One reason is the sensitivity of the substrate towards the impinging electron beam in commercial standard LEED-systems. We have set up a channel-plate LEED system [27,28] which operates with electron currents in the nA regime, with which we shall tackle this problem in the near future. It is very likely that the present  $p(2 \times 2)$  reconstruction is of the octopolar type predicted earlier and schematically shown in Fig. 1b. For a more detailed discussion of this aspect see Ref. [6].

The patterns are rather diffuse but various at-

tempts to find optimal preparation conditions to form a well ordered structure failed. The  $p(2 \times 2)$  fractional spot intensity is sensitive to the back ground pressure, while the integral order structure is rather insensitive. In fact, after several hours the fractional  $p(2 \times 2)$  spots are strongly attenuated. The same result can be obtained if we expose the  $p(2 \times 2)$  structure to 0.3 L  $H_2O$ . The process is completely reversible and may be cycled. Therefore, it is experimental fact that the NiO(111) surface reconstructs after the OH covered surface has been heated to 600 K. This reconstruction does not lead to a well ordered surface as indicated by the large spot widths. Nevertheless, the process is perfectly reproducible in every preparation cycle. The reconstruction can be lifted upon exposure to water, and this process is also reversible.

It is quite probable that the sensitivity of surface structure to the presence of water on the surface has general consequences for the reactivity of the oxide surfaces. We have demonstrated before [5] that the number of adsorbed NO molecules – as monitored via thermal desorption – increases by about a factor of three after desorption of the hydroxyl groups. In addition, high temperature desorption of NO (above 400 K) is observed indicating the reaction of adsorbed NO, tentatively to  $NO_2$  for example. In this sense, water steers the reactivity of the oxide surface as a function of surface temperature where the temperature for OH desorption sets the threshold to activate the sample, and in particular the polar surface patches. Whether this observation is relevant to catalytic processes, is not clear at present but there are indications that the catalytic activity of NiO catalysts prepared through topotactic dehydration of  $Ni(OH)_2$ , i.e. forming crystallites with (111) orientation [29], is strongly influenced by water in the gas phase and on the sample.

### 3.2. CoO(111) / Co(0001)

Fig. 3b shows the LEED patterns of the clean Co(0001) surface exhibiting sharp spots in contrast to the oxidized surface which show the more diffuse LEED spots typical for a CoO(111) surface formed via oxidation [14,15,30]. The situation is thus very similar to the one encountered for NiO(111). Fig. 6 collects the HREEL spectra in the vibrational regime

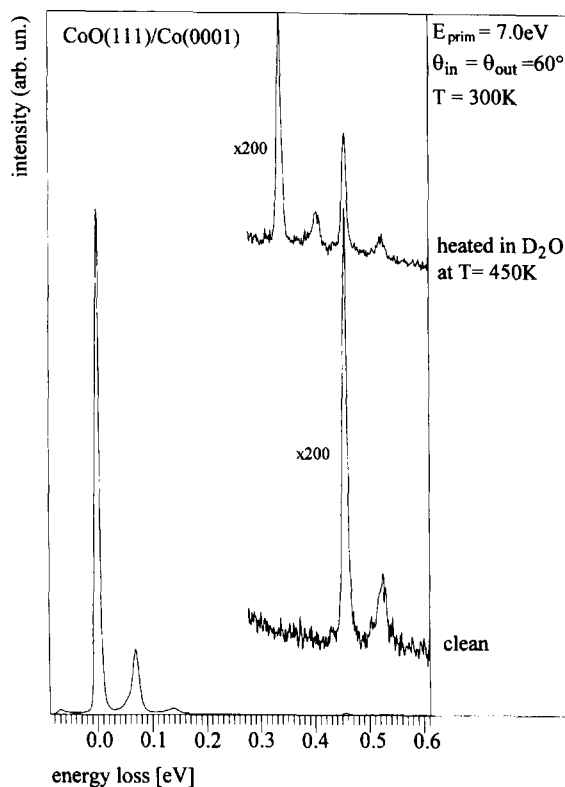


Fig. 6. HREEL spectrum of the CoO(111) surface in the range of surface vibration. (a) as prepared, (b) after heating in  $D_2O$ .

indicating the presence of hydroxyl groups as the only observable adsorbed chemical species. The intense features are again the Fuchs–Kliwer phonon losses. The additional feature about 70 meV above the OH loss is due to a combination vibration combining OH and phonon losses. As in the case of the NiO(111) surface it is possible to exchange the hydroxyl groups partly via  $D_2O$  exposure at higher temperature. This is demonstrated in the upper trace of Fig. 6 where a second set of losses, shifted by the appropriate value expected from the isotope exchange is found. The conclusion from the EELS investigation is very similar to the one drawn for NiO(111): CoO(111) is covered with hydroxyl groups in order to stabilize the unstable clean (111) rock salt type surface. The next obvious step is to try and remove the hydroxyl groups by a heat treatment as in the case of the NiO(111) surface. However, so far we have failed to do so without partly destroying the

oxide film. This is the main reason why we have been unsuccessful so far to observe the  $p(2 \times 2)$  reconstruction of the  $\text{CoO}(111)$  surface.

### 3.3. $\text{FeO}(111) / \text{Fe}(110)$

The iron oxide system has been studied in detail in the past [7–10,13,16–23]. Out of the many results we would like to mention the observation that the  $\text{FeO}(111)$  film, prepared epitaxially on a  $\text{Pt}(111)$  surface, exhibits a reconstruction to form a  $p(2 \times 2)$  LEED pattern [7–10]. Weiß et al. [7,10] have demonstrated that at the surface a  $\text{Fe}_3\text{O}_4$  layer forms which happens to have the proper lattice parameters to induce a  $p(2 \times 2)$  LEED pattern. The same situation is encountered when a bulk  $\text{Fe}_2\text{O}_3$  single crystal is sputtered and heated [10,11]. Again a  $p(2 \times 2)$  superstructure forms which is also due to the formation of a thin  $\text{Fe}_3\text{O}_4$  layer at the surface. The driving force for this surface reconstruction may be found in the phase diagram of the Fe–O system [12]. The thermodynamically stable phase under the given oxygen pressure and the limited Fe supply is the  $\text{Fe}_3\text{O}_4$  phase. However, if the films, discussed above, were not grown on top of a  $\text{Pt}(111)$  surface but rather on a Fe surface, i.e. on a  $\text{Fe}(110)$  surface, the situation is different. Simply, the high iron concentration in the system [18,31] will shift the equilibrium towards the FeO system according to:

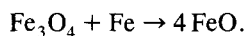


Fig. 3c shows the LEED pattern when a  $\text{Fe}(110)$  crystal is oxidized as discussed in the experimental part. It clearly shows a  $p(2 \times 2)$  LEED pattern suggesting for the first glance the formation of a  $\text{Fe}_3\text{O}_4$  overlayer as in the case of the film on the  $\text{Pt}(111)$  surface. The EELS spectrum (not shown) indicates very little OH on the surface, only of the magnitude seen for the reconstructed  $\text{NiO}(111)$  surface. However, while  $\text{H}_2\text{O}$  would remove the reconstruction in the NiO case, in the case of ironoxide we may actually grow a thick  $\text{H}_2\text{O}$  film on the surface. This is revealed by XPS measurements. Fig. 7 shows the O 1s spectra before and after exposure to  $\text{H}_2\text{O}$ . The very tiny shoulder or rather asymmetry on the O 1s line corroborates the conclusion from EELS that very little OH is on the surface. If we expose the

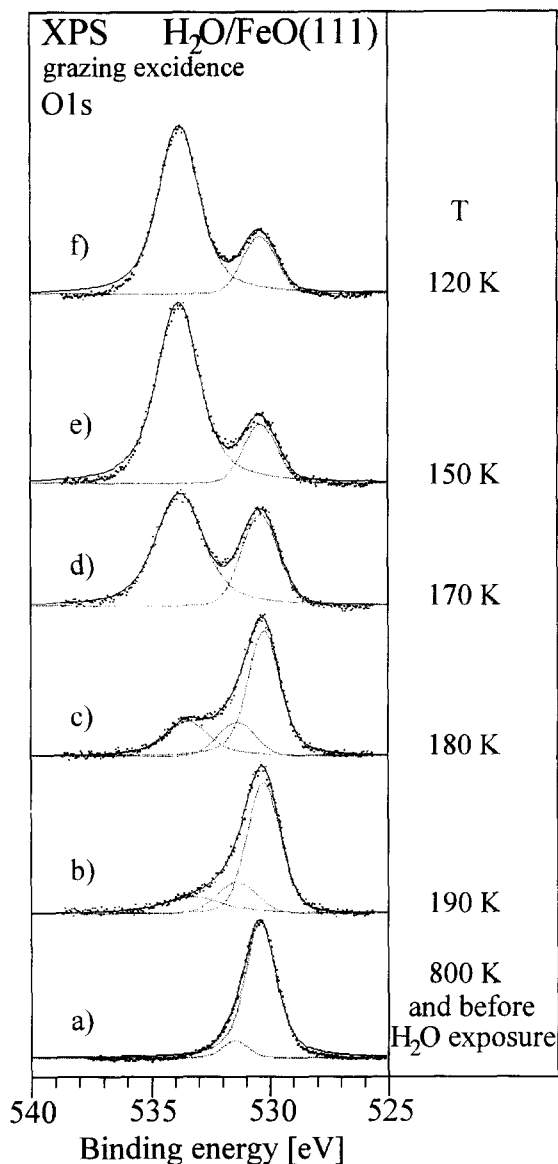


Fig. 7. O 1s spectra of the  $\text{FeO}(111)$  films as prepared. (a) clean film, (b)–(f) ice film on  $\text{FeO}(111)$  prepared at  $T = 120$  K heated to various surface temperatures.

surface to  $\text{H}_2\text{O}$  we can see the  $\text{H}_2\text{O}$  layer growing by watching the O 1s peak clearly removed from the O 1s peak due to the oxide. Heating of the system, attenuates the the  $\text{H}_2\text{O}$  peak gradually and there is no stable or metastable intermediate situation which could be assigned to a surface containing a larger



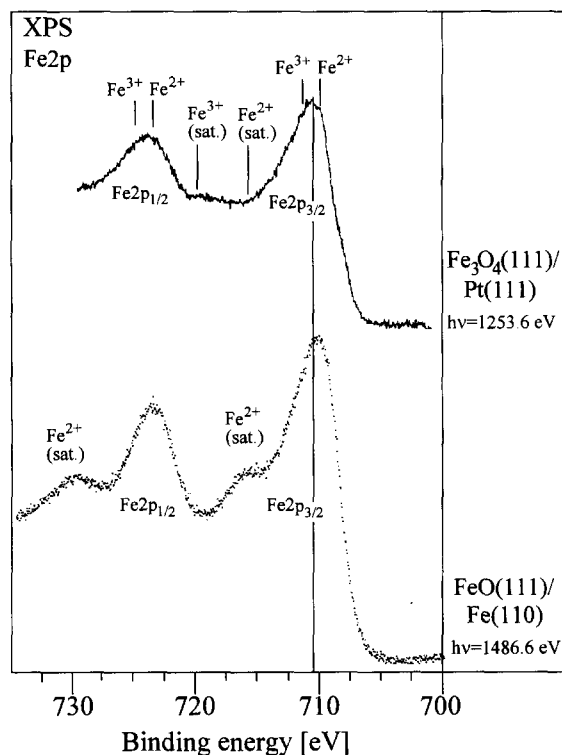


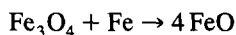
Fig. 8. Fe 2p<sub>3/2</sub> spectra of the FeO(111) film as prepared on a Fe(110) surface. In comparison we show the corresponding spectrum of a Fe<sub>3</sub>O<sub>4</sub> film as prepared on Pt(111) according to Weiß et al. [7,10].

amount of OH. A clue, as to whether the surface is a Fe<sub>3</sub>O<sub>4</sub> or rather a FeO overlayer may be reached if we investigate the Fe 2p photoemission spectra (Fig. 8). There are clear differences to be expected on the basis of the literature data: the Fe 2p spectra of Fe<sup>2+</sup> which is the only oxidation state in FeO exhibit strong satellite features while the mixed valence compound Fe<sub>3</sub>O<sub>4</sub> does not exhibit intense satellites and a slight shift of the main ionization line. On the basis of this fingerprint FeO and Fe<sub>3</sub>O<sub>4</sub> may be differentiated. Fig. 8 compares the XPS spectra of the Fe<sub>3</sub>O<sub>4</sub> film grown on Pt(111) as reported by Weiß et al. and our present data. It is quite obvious without any further, more detailed analysis that the film grown on the Fe(110) surface contains Fe<sup>2+</sup> as in FeO while the system grown on the Pt(111) surface is, indeed, a Fe<sub>3</sub>O<sub>4</sub> layer. We presently think

that this finding is not a contradiction. On the contrary, it corroborates the idea that thermodynamics drives the reconstruction and that the thin film communicates with the bulk material as alluded to above.

#### 4. Summary and conclusions

We have shown that the NiO(111) surface reconstructs as predicted by the mainly electrostatic model taking the electronic structure of NiO as basically ionic. The reconstruction is driven by the presence of hydroxyl groups on the surface, i.e. removing OH destabilizes the surface and induces the reconstruction. It is not proven but very likely that the reconstruction is of the octopolar type. The situation is somewhat more complicated for the other rock salt type oxides, i.e. CoO(111) and FeO(111). In fact, CoO(111) may be grown in the same manner as NiO(111) and also exhibits very similar properties and OH concentrations, but the system is not stable enough to tolerate the temperature needed for OH removal. FeO(111) on the other hand, if it is grown on a Fe(110) single crystal surface, does not contain larger amounts of OH on the surface and it does not want to dissociate H<sub>2</sub>O as easily as NiO(111). Indeed, the FeO(111) surface in our case does not form a Fe<sub>3</sub>O<sub>4</sub> overlayer but rather remains of the FeO type as shown via the Fe 2p XPS analysis. It seems that the surface is stable in the “reconstructed” form. Whether this reconstruction, which leads to the same LEED pattern as the one observed for NiO is of the octopolar type is not clear at the moment. It is pointed out that the formation of an FeO film at the surface is in line with the thermodynamics as long as we consider the supporting metal. Therefore the finding here is not a contradiction to the results of Weiß et al. [7–10] for an ironoxide film on Pt(111). They have shown that in the latter case a Fe<sub>3</sub>O<sub>4</sub> film is formed at the surface. If we invoke the equilibrium



in the present case, with Fe, being the large Fe reservoir of the support, it is quite obvious that under the preparation conditions the system resides on the right hand side of the equilibrium.

## Acknowledgements

Our work has been supported by: Deutsche Forschungsgemeinschaft and Ministerium für Wissenschaft und Forschung des Landes Nordrhein-Westfalen as well as the Fonds der Chemischen Industrie. We thank these institutions for their support.

## References

- [1] R. Lacman, *Colloq. Int. C.N.R.S.* 152 (1965) 195.
- [2] D. Wolf, *Phys. Rev. Lett.* 68 (1992) 3315.
- [3] H.-J. Freund and E. Umbach, Eds., *Adsorption on Ordered Surfaces of Ionic Solids and Thin Films*, Vol. 33 of Springer Series in Surface Science (Springer, Berlin, 1993).
- [4] F. Winkelmann, S. Wohlrab, J. Libuda, M. Bäumer, D. Cappus, M. Menges, K. Al-Shamery, H. Kuhlenbeck and H.-J. Freund, *Surf. Sci.* 307–309 (1994) 1248.
- [5] D. Cappus, C. Xu, D. Ehrlich, B. Dillmann, C.A. Ventrice, K. Al-Shamery, H. Kuhlenbeck and H.-J. Freund, *Chem. Phys.* 177 (1993) 533.
- [6] F. Rohr, K. Wirth, J. Libuda, D. Cappus, M. Bäumer and H.-J. Freund, *Surf. Sci.* 315 (1994) 2977.
- [7] W. Weiß, A.B. Boffa, J.C. Demply, H.C. Gattoway, M.B. Salmeron and G.A. Somorjai, in Ref. [3].
- [8] A. Barbieri, W. Weiß, M.A. van Hove and G.A. Somorjai, *Surf. Sci.* 302 (1994) 259.
- [9] G.A. Vurenco, M.B. Salmeron and G.A. Somorjai, *Surf. Sci.* 201 (1988) 129.
- [10] W. Weiß, A. Barbieri, M.A. Van Hove and G.A. Somorjai, *Phys. Rev. Lett.* 71 (1993) 1848.
- [11] R.J. Lad and V.E. Henrich *Surf. Sci.* 193 (1988) 81.
- [12] A. Muan, *Am. J. Sci.* 256 (1958) 171.
- [13] E. Neuhaus, *Diplomarbeit, Ruhr-Universität Bochum*, 1994.
- [14] A. Ignatiev, B.W. Lee and M.A. Van Hove, *Proc. 7th Int. Vac. Congr. and 3rd Int. Conf. Solid Surf.*, Vienna (1977) p. 1733.
- [15] R.B. Mays and M.W. Roberts, *J. Catal.* 49 (1977) 216.
- [16] A.J. Pignocco and G.E. Pellisier, *Surf. Sci.* 7 (1967) 261.
- [17] C. Leygraf and S. Ekelund, *Surf. Sci.* 40 (1973) 609.
- [18] M. Langell and G.A. Somorjai, *J. Vac. Sci. Technol.* 21 (1982) 858.
- [19] S. Masuda, Y. Harada, H. Kato, K. Yagi, T. Komeda, T. Miyano, M. Onchi and Y. Sakisaka *Phys. Rev. B* 37 (1988) 8088.
- [20] V.S. Smentkowski and J.T. Yates, Jr., *Surf. Sci.* 232 (1990) 113.
- [21] F. Portele, *Z. Naturforsch. A* 24 (1969) 1268.
- [22] G. Pirug, G. Broden and H.P. Bonzel, *Surf. Sci.* 94 (1980) 323.
- [23] C.R. Brundle, *IBM J. Res. Dev.* 22 (1978) 235.
- [24] M. Bäumer, D. Cappus, H. Kuhlenbeck, H.-J. Freund, A. Brodde and H. Neddermeyer, *Surf. Sci.* 253 (1991) 116.
- [25] A. Freitag, V. Staemmler, D. Cappus, C.A. Ventrice, Jr., K. Al-Shamery, H. Kuhlenbeck and H.-J. Freund, *Chem. Phys. Lett.* 210 (1993) 10.
- [26] A. Freitag and V. Staemmler, private communication; A. Freitag, PhD Thesis, Ruhr-Universität Bochum, in preparation.
- [27] F. Rohr, PhD Thesis, Ruhr-Universität Bochum, in preparation.
- [28] K. Wirth, *Diplomarbeit, Ruhr-Universität Bochum*, 1993.
- [29] B. Egersdörfer and H. Papp, private communication.
- [30] M. Haßel, PhD Thesis, Ruhr-Universität Bochum, in preparation.
- [31] T. Migano, Y. Sakitata, T. Komeda and M. Onchi, *Surf. Sci.* 169 (1986) 197.